

Off-axis electron holography for imaging the magnetic behavior of vortex-state minerals

TREVOR P. ALMEIDA¹, ADRIAN R. MUXWORTHY², WYN WILLIAMS³, TAKESHI KASAMA⁴, ANDRÁS KOVÁCS⁵ AND RAFAL E. DUNIN-BORKOWSKI⁵

¹ SUPA, School Of Physics And Astronomy, University Of Glasgow, Glasgow G12 8DQ, U.K.

² Department Of Earth Science And Engineering, South Kensington Campus, Imperial College London, London SW7 2AZ, U.K.

³ School Of Geosciences, University Of Edinburgh, Edinburgh EH9 3JW, U.K.

⁴ National Centre For Nano Fabrication And Characterization, Technical University Of Denmark, Dk-2800 Kgs. Lyngby, Denmark.

⁵ Ernst Ruska-Centre For Microscopy And Spectroscopy With Electrons And Peter Grünberg Institute, Forschungszentrum Jülich, 52425 Jülich, Germany.

INTRODUCTION

Transmission electron microscopy (TEM) is a widely-used multi-purpose characterization technique that allows for the localized investigation of thin, electron-transparent samples.

Most conventional TEMs are used to characterize the chemistry, morphology and structure of materials over a range of length scales, with modern spherical and chromatic aberration corrected TEMs providing interpretable spatial resolutions approaching ~ 50 picometers.

More specialized capabilities of TEMs allow for the imaging and measurement of electrostatic potentials and magnetic fields within and around samples with nanometer spatial resolution. TEM-based phase contrast techniques that can be used for such measurements include Lorentz imaging¹, off-axis electron holography (EH)² and differential phase contrast (DPC) imaging in scanning TEM³. These techniques are sensitive to the phase of the electron beam that has passed through the sample and hence can be used to image nanoscale magnetism.

Off-axis EH is arguably the most powerful of these methods for imaging magnetic induction within three-dimensional (3D) nanoscale materials, as DPC imaging is usually applied to samples of relatively uniform thickness and Lorentz imaging is mostly used to reveal and examine magnetic domain walls.

Off-axis EH involves the use of an electron biprism in a TEM to split and then overlap an electron beam, part of which travels through a region of interest in a sample, resulting in the formation of an interference pattern (or hologram). The positions of the interference fringes record phase information about the part of the electron wave that passed through the sample.

This phase information can be used to reconstruct the local projected in-

plane magnetic induction within and around the sample.

Off-axis EH has been used to investigate the magnetic properties of a wide range of nanostructured materials, including nanoparticle assemblies⁴, heterostructured minerals⁵, meteorites⁶, nanodisks⁷, mesocrystals⁸, nanorings⁹, nanowires¹⁰, skyrmions¹¹, spin valves¹², superlattices¹³ and twin-induced nanodomains¹⁴. Many of these materials are candidates for applications that range from magnetic data storage to geophysics.

An area of research in which off-axis EH has been employed is the investigation of magnetic signals in rocks (paleomagnetism), in which nanoscale magnetic grains can store information from the time of rock formation¹⁵. The magnetic states that are found in natural systems are often complex and highly non-uniform and are ideally suited to characterization using off-axis EH.

Paleomagnetists are interested in the stability of the magnetic signals over geological timescales, during which the magnetic carriers are susceptible to oxidation and phase transformations¹⁶, as well as to thermal fluctuations^{17,19}. Hence, it is of interest to establish how the recorded magnetic signal is affected by both chemical alteration and temperature.

This article focuses on the combination of modern *in situ* TEM techniques with off-axis EH to visualize dynamic magnetic signals in the most important magnetic mineral on Earth, magnetite (Fe₃O₄), in one of the most commonly occurring magnetic domain states found in rocks, the vortex state²⁰.

MATERIALS AND METHODS

Sample details: Instead of using Fe₃O₄ samples found in nature, which often contain impurities and would require destructive sample preparation for TEM analysis, a synthetic Fe₃O₄ powder was

investigated. The Fe₃O₄ grains in this sample act as good representations of 3D magnetic carriers found in rocks and have large exposed surface areas that are favorable for performing *in situ* oxidation experiments.

Fe₃O₄ particles of diameter < 250 nm (hydrothermally synthesized by Nanostructured and Amorphous Materials, USA) were cleaned with acetone and centrifuged for six minutes at 6000 rpm. For the purpose of environmental and *in situ* TEM investigations, the particles were dispersed in distilled water or ethanol using an ultrasonic bath, before deposition onto Aduro E-chips (Protochips, USA) or Wildfire E-chips (DENSO Solutions, The Netherlands).

Off-axis EH: The off-axis electron holograms that are presented below were acquired at 300 kV using FEI Titan 80-300 TEMs equipped with rotatable electron biprisms and Lorentz mini-lenses, as shown in Fig. 1a. These microscopes can be used to record off-axis electron holograms in magnetic-field-free conditions (in a residual field of ≤ 0.2 mT).

Imaging was performed at the National Centre for Nano Fabrication and Characterization (DTU Nanolab), Technical University of Denmark, and the Ernst Ruska-Centre for Microscopy and Spectroscopy with Electrons (ER-C), Forschungszentrum Jülich, Germany.

Off-axis electron holograms of Fe₃O₄ grains (Fig. 1b) were recorded using either a charged-coupled device camera or a Gatan K2 Summit direct detection camera. The total phase shift recorded using off-axis EH is sensitive to both the electrostatic potential and the in-plane component of the magnetic induction within and around the specimen, according to the equation

$$\varphi(x, y) = \varphi_e + \varphi_m = C_E \int V(x, y, z) dz - C_B \int A_z(x, y, z) dz,$$

where $C_E = \pi\gamma/\lambda U^*$ is an interaction constant that depends on



BIOGRAPHY

Trevor Almeida completed his Ph.D. and an EPSRC Doctoral Prize Fellowship focusing on the synthesis and characterization of metal oxide nanoparticles at the University of Nottingham. He spent four years as a research associate at Imperial College London, including one-year research visits to the National Centre for Nano Fabrication and Characterization in Denmark and the Ernst Ruska-Centre for Microscopy and Spectroscopy with Electrons in Germany. He is currently a Lord Kelvin Adam Smith Research Fellow at the University of Glasgow, focusing on visualizing dynamic magnetism in nanostructures using a range of *in situ* TEM techniques.

ABSTRACT

The advanced transmission electron microscopy (TEM) technique of off-axis electron holography (EH) can be used to image magnetic fields within and around nanoscale materials. Here, we show how combining off-axis EH with the modern *in situ* TEM capabilities of controlled heating in vacuum or a reactive gas environment can provide spatially resolved dynamic information about magnetic vortex states in Fe₃O₄ grains. Our experiments reveal that *in situ* oxidation can change the strengths and directions of magnetic vortices in individual Fe₃O₄ grains or groups of interacting grains. In contrast, during *in situ* heating we observe that magnetic vortices in Fe₃O₄ grains are remarkably stable to thermal effects, with smaller Fe₃O₄ grains exhibiting dynamic magnetic behavior at temperatures approaching their Curie temperature. The accurate imaging of three-dimensional dynamic magnetism in such nanostructures promises to be realized in the future through advances in *in situ* TEM holders and the analysis of experimental results using micromagnetic modeling.

ACKNOWLEDGEMENTS

We are grateful for support from the Engineering and Physical Sciences Research Council (EP/P50354X/1), the Natural Environment Research Council (NE/J020966/1 and NE/J020966/1) and the European Research Council (Advanced Grant 320832).

CORRESPONDING AUTHOR

trevor.almeida@glasgow.ac.uk

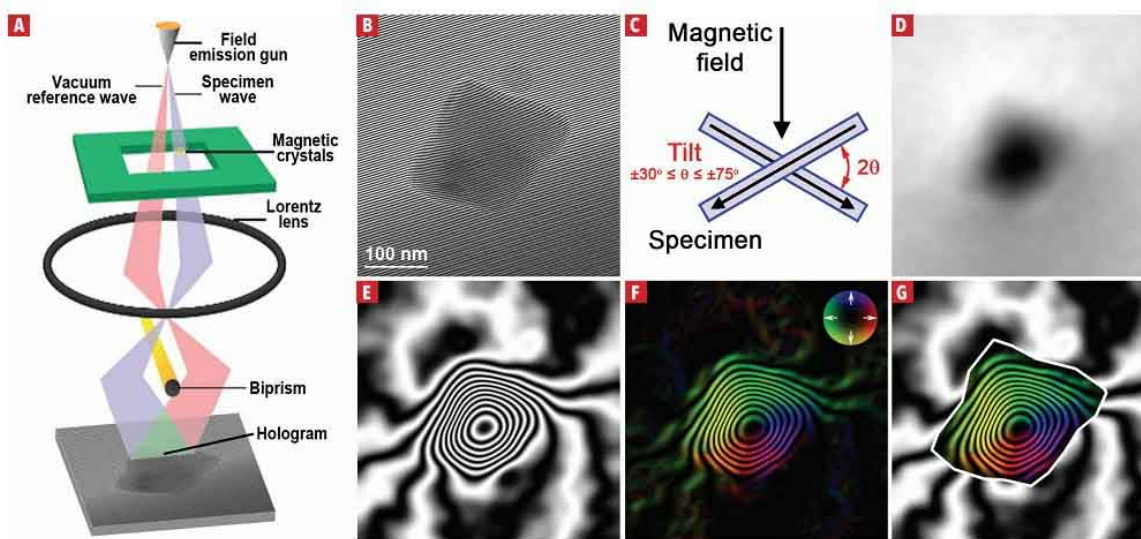


FIGURE 1 Experimental setup used to record off-axis electron holograms and data processing to produce magnetic induction maps. (a) Schematic diagram showing how the application of a voltage to an electron biprism results in the overlap of sample and reference waves, producing interference fringes. (b) Electron hologram of a Fe_3O_4 grain (~ 250 nm diameter), displaying well-resolved interference fringes. (c) Schematic illustration of the use of sample tilting to reverse the in-plane component of the magnetization, in order to separate the MIP contribution to the total phase shift. (d) Magnetic contribution to the total phase shift. (e) Cosine of a chosen integer times the magnetic contribution to the phase shown in (d) to produce contours with a spacing of 0.53 radians. (f) The addition of color shows the direction of the projected in-plane magnetic induction in the Fe_3O_4 grain, according to the color wheel (inset). (g) The final magnetic induction map visually shows the strength and direction of the magnetic signal in the Fe_3O_4 grain and the stray magnetic field.

the microscope accelerating voltage ($C_e = 6.53 \text{ V}^{-1} \mu\text{m}^{-1}$ at 300 kV), λ is the electron wavelength, γ is the relativistic Lorentz factor and U^* is the relativistically corrected accelerating potential²¹, while the constant $C_g = \pi/\phi_0$, where ϕ_0 is the magnetic flux quantum $h/2e = 2.07 \times 10^3 \text{ T nm}^2$, is independent of electron energy.

In order to isolate the magnetic contribution to the recorded phase shift, the direction of magnetization in each particle was reversed *in situ* in the TEM by tilting the sample to equal but opposite angles between $\pm 30^\circ$ and $\pm 75^\circ$.

The objective lens was then turned on to apply a saturating magnetic field

of 1.5 to 2 T to the sample parallel to the direction of the electron beam, as shown in Fig. 1c.

Finally, the objective lens was turned off and the sample tilted back to 0° for electron hologram acquisition in magnetic-field-free conditions with the Fe_3O_4 particles in magnetic remanent states, i.e., the particles were initially induced with a saturation isothermal remanence at room temperature.

By taking differences between phase images reconstructed from electron holograms that had been recorded with the particles magnetized in opposite directions, the mean inner potential (MIP) contribution to the phase could be subtracted from the

total recorded phase, thereby isolating the desired magnetic contribution to the phase (Fig. 1d). For the construction of magnetic induction maps, the cosine of a chosen integer multiplied by the magnetic contribution to the phase shift was used to generate magnetic phase contours (Fig. 1e).

Colors were added to the contours to show the direction of the projected in-plane magnetic induction (Fig. 1f), as denoted by a color wheel (Fig. 1f, inset). The original off-axis electron hologram was then used to create a mask to visually separate the recorded magnetic signal within the Fe_3O_4 grain from the surrounding stray magnetic field (Fig. 1g).

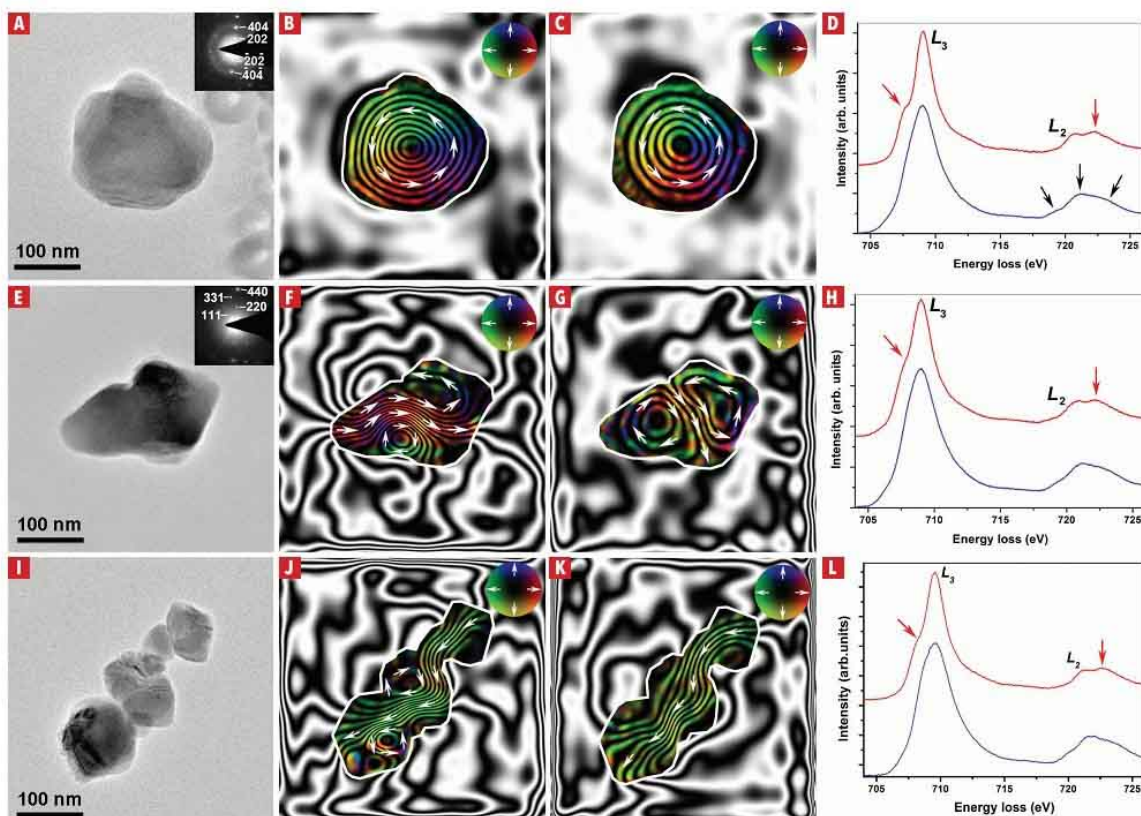


FIGURE 2 Visualized effect of oxidation on the magnetization of Fe_3O_4 particles. (a, e, i) Bright-field TEM images acquired before *in situ* heating to 700°C in 9 mbar of O_2 for 8 hours in an ETEM. (b, c, g, j, k) Magnetic induction maps obtained from the magnetic contribution to the phase shift reconstructed from off-axis electron holograms recorded (b, f, j) before and (c, g, k) after *in situ* heating. (d, h, l) Corresponding EEL spectra showing the Fe $2p$ $L_{2,3}$ edge recorded from the Fe_3O_4 particles before (blue) and after (red) annealing in the ETEM. Black arrows highlight three differing intensities from the mixed-valence compound of Fe_3O_4 , while red arrows highlight the formation of pre- and post-peaks, which are indicative of oxidation towards $\gamma\text{-Fe}_2\text{O}_3$.

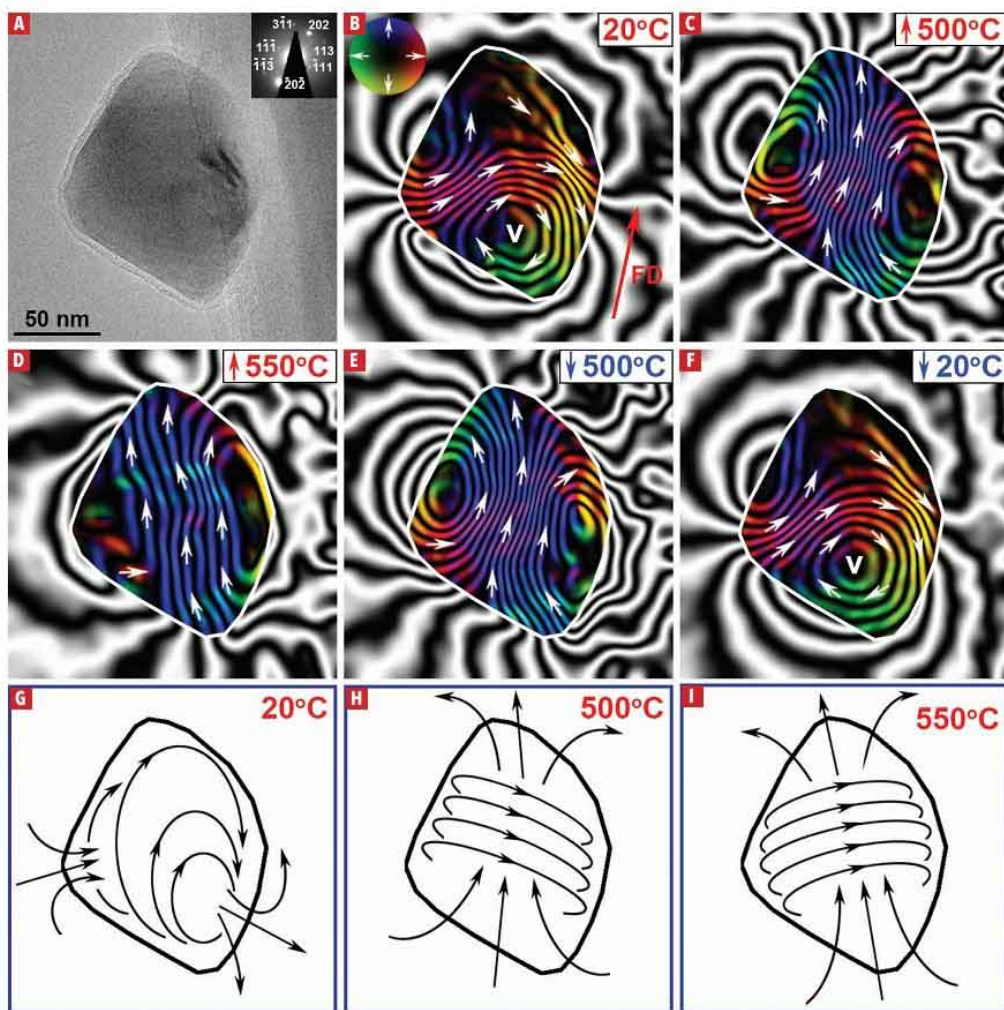


FIGURE 3 Off-axis electron holography of the thermomagnetic behavior of a small Fe_3O_4 grain. (a) Bright-field TEM image of the individual Fe_3O_4 grain (~150 nm in diameter), with an associated electron diffraction pattern inset. (b-f) Magnetic induction maps reconstructed from off-axis electron holograms recorded (b) at 20°C (with the red arrow, labelled FD, showing the direction of the in-plane component of the saturating magnetic field used to induce remanence) and (c-f) during *in situ* heating to (c) 500°C and (d) 550°C and subsequent cooling to (e) 500°C and (f) 20°C. The letter “v” identifies the center of a magnetic vortex. (g-i) Schematic representations of the proposed 3D forms of the magnetic vortex states that are observed experimentally in projection at (g) 20°C, (h) 500°C and (i) 550°C.

Environmental TEM for *in situ* oxidation: *In situ* oxidation of Fe_3O_4 particles was studied using an FEI Titan E-Cell TEM with a C_2 corrector on the objective lens, operated at 300 kV, in 9 mbar of O_2 , at elevated temperature, using a Protochips heating holder (DTU Nanolab).

The elevated temperature of 700 °C was chosen to help to compensate for the lower pressure used during ETEM experiments than ambient pressure conditions in nature. Electron energy-loss spectroscopy (EELS) analysis was performed with a spectral resolution of ~ 0.03 eV using a monochromator, in order to provide information about the oxidation state of the sample.

All TEM imaging and EELS acquisition was performed on grains that were stabilized under high vacuum conditions at ambient temperature, with *in situ* oxidation performed in the absence of the electron beam to avoid any sample degradation through electron beam / material interaction during annealing.

Thermal stability of magnetic remanent states: Fe_3O_4 particles were initially pre-heated *in situ* in the TEM to 700°C in vacuum to evaporate any remaining water and to alleviate any possible strain induced during particle synthesis. In order to record initial

room temperature magnetic states, electron holograms were acquired using the methodology described above. Electron holograms were then recorded in magnetic-field-free conditions during *in situ* heating in 50 or 100 °C intervals up to 550 or 600 °C and again upon cooling using a single tilt DENSO solutions heating holder (ER-C).

Magnetization reversal was performed by turning on the objective lens with the specimen tilted to $\pm 75^\circ$ at each temperature in order to determine the MIP contribution to the phase, which was then subtracted from the unwrapped total phase shift acquired at each temperature during the initial heating experiment, in order to construct magnetic induction maps of magnetic remanent states at each temperature.

RESULTS / DISCUSSION

Effect of oxidation: Figure 2 illustrates the effect of oxidation on the magnetization of individual Fe_3O_4 grains assessed using TEM, EELS and reconstructed magnetic induction maps. Figure 2a shows a bright-field TEM image of an Fe_3O_4 grain (~200 nm in diameter) prior to induced oxidation. EELS analysis of the Fe 2p $L_{2,3}$ edge in the region 704 – 726 eV

(blue spectra, Fig. 2d) confirmed the assignment of pure Fe_3O_4 .

The L_2 edge for this sample shows the typical shape of a mixed valence compound, with three visible features with differing intensities (Fig. 1c, black arrows), while the almost shapeless L_3 edge is attributed to the combined spectral contributions of Fe^{2+} at octahedral B sites and Fe^{3+} at both tetrahedral A and octahedral B sites, as compared with other mixed iron oxides^{22,23}.

The corresponding magnetic induction map shown in Fig. 2c contains evenly-spaced magnetic contours from the surface to the center of the grain, flowing in a counter-clockwise direction (denoted using arrows), characteristic of a vortex state.

After exposure to 9 mbar of O_2 at 700°C for 8 h in the ETEM, fine features develop in the form of a small pre-peak on the L_3 edge and a post-peak on the L_2 edge (Fig. 2d, red spectra and arrows), indicative of a change in Fe oxidation state towards $\gamma\text{-Fe}_2\text{O}_3$ or $\alpha\text{-Fe}_2\text{O}_3$ ^{24,26}.

The spacings between the phase contours in the corresponding magnetic induction map (Fig. 2c), which again flow in a counter-clockwise direction, are observed to widen, most markedly towards the particle

edge, indicating an oxidation-induced change in magnetism. Figure 2e shows a bright-field TEM image of an elongated (~250 nm long, ~150 nm wide) Fe_3O_4 grain, supported by a complementary EEL spectrum in Fig. 2h (blue). A corresponding magnetic induction map in Fig. 2f reveals closely-spaced magnetic contours flowing from left to right through the elongated particle, interacting with a small vortex located at the bottom of the grain, in addition to a stray magnetic field.

In a similar manner to the Fe_3O_4 grain shown in Fig. 2b-d, the additional development of a small pre-peak on the L_3 edge and as post-peak on the L_2 edge of the corresponding EEL spectrum (Fig. 2h, red arrows) are again strong indicators of the effects of progressive oxidation towards $\gamma\text{-Fe}_2\text{O}_3$ or $\alpha\text{-Fe}_2\text{O}_3$. The associated magnetic induction map (Fig. 2g) contains two vortices with widened phase contour spacings flowing in opposite directions around a central transverse axis, again indicating an oxidation-induced change in magnetism.

Figure 2i shows a bright-field TEM image of a group of Fe_3O_4 grains, once more confirmed by an EEL spectrum (blue) in Fig. 2l. The pre-oxidation magnetic induction map (Fig. 2j) reveals magnetic interactions between the grains, with closely-spaced magnetic contours flowing from the top right through the grains in a dog-leg fashion to the bottom left, interacting with several vortices. The EEL spectra in Fig. 2l (red) confirm oxidation through the development of pre-peaks (arrowed), while the associated magnetic induction map (Fig. 2k) shows a widening of the magnetic contours, which flow from top right to bottom left in a more direct manner, with no vortices present.

This combined ETEM and off-axis EH investigation provides a visual representation of the effects of accelerated chemical oxidation on the direction and intensity of the magnetization of vortex-state Fe_3O_4 particles. The development of additional peaks in the Fe 2p $L_{2,3}$ edges provides evidence for the process of oxidation²⁴. The widening of magnetic phase contours around the vortex observed in the oxidized isotropic Fe_3O_4 grain shown in Fig. 2c, compared to its initial state (Fig. 2d), demonstrates that chemical alteration leads to a loss of magnetization intensity.

In addition, clockwise rotation of the central magnetic contours, from the major axis of the elongated Fe_3O_4 particle (Fig. 2f) to a transverse axis (Fig. 2g), demonstrates the strong effect of oxidation on magnetization direction, an effect that was previously considered to be dominated by shape anisotropy. It is suggested that sharp particle tips and large exposed areas in groups of particles are more susceptible to oxidation towards the less magnetic $\gamma\text{-Fe}_2\text{O}_3$ phase, resulting in alteration of the crystallographic phase distribution to lower aspect ratio

Fe_3O_4 cores in the case of Fig. 2g, or to an Fe_3O_4 core that extends through the particles in Fig. 2k, prompting a shift towards lower energy and a more favorable direction of magnetization.

The magnetic induction maps in Fig. 2 show the effect of oxidation on remanent saturation magnetization. The sample was transferred between different TEMs, each with separate *in situ* oxidation and off-axis EH capabilities. The development of modern gas cell heating TEM chips, such as those from DENSolutions, Hummingbird or Protocips, allows for direct measurement of the true effect of chemical alteration on remanent magnetic states through the systematic acquisition of electron holograms in magnetic-field-free conditions. This is evidenced through the investigation of thermal effects on the true remanent magnetic behavior of Fe_3O_4 grains presented in the next section.

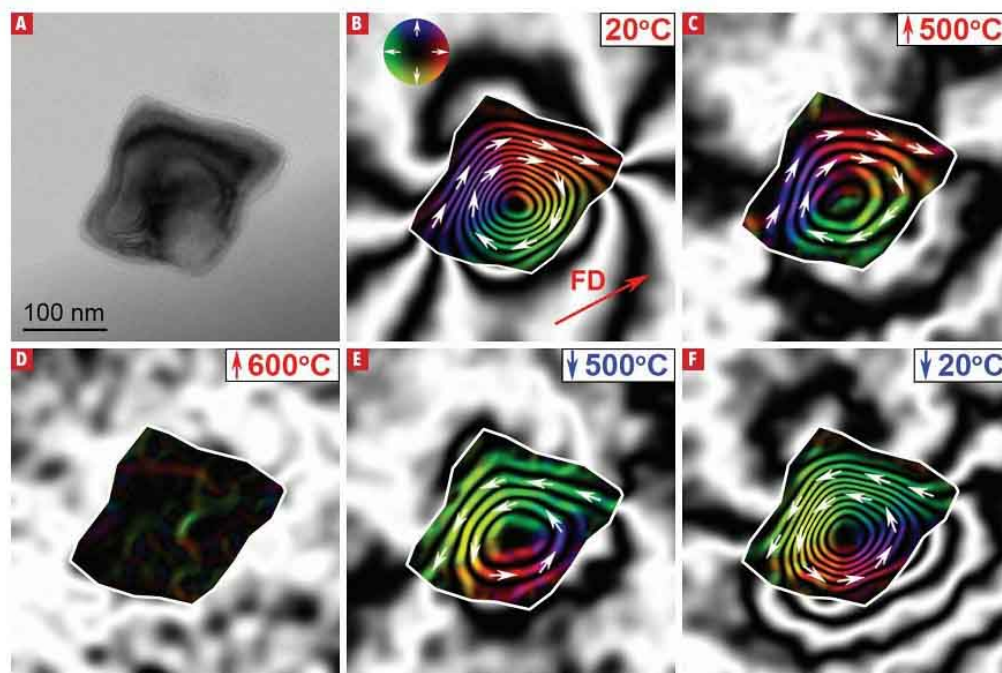
Effect of temperature: The thermomagnetic behavior of a small Fe_3O_4 grain, which was heated from 20 to 550 °C and then cooled back to 20 °C, is shown in Fig. 3. Figure 3a shows a bright-field TEM image of the Fe_3O_4 grain, which has a length of ~150 nm along its long diagonal axis. Figure 3b shows a magnetic induction map of the Fe_3O_4 grain obtained from off-axis electron holograms recorded at room temperature (20 °C).

The induction map shows that the magnetization flows generally from left to right and interacts with a small vortex core (denoted v), in addition to a component of stray magnetic field. A schematic diagram of the likely 3D form of this vortex state is shown in Fig. 3g. However, the vortex state at remanence changes markedly when the temperature is increased to 500 °C (Fig. 3c), with the magnetic phase contours narrowing, aligning along the long diagonal axis and curving away from this axis at the top and bottom of the grain.

A further increase in temperature to 550 °C (Fig. 3d) results in a widening of the magnetic phase contours, which become more closely aligned with the long diagonal axis. The magnetic states observed at 500 and 550 °C could be misinterpreted as uniformly magnetized or single domain (SD) states. However, because the magnetic flux loops on either side of the central magnetic contours are contained within the Fe_3O_4 grain, they are likely to be magnetic vortex states that are viewed edge-on^{27,28}, as shown in Figs 3h and 3i.

On cooling to 500 °C, the magnetic induction map (Fig. 3e) is similar to that in Fig. 3c, finally recovering the initial magnetic state (Fig. 3f) at 20 °C, similar to its state prior to heating (Fig. 3b).

In a similar manner to that observed in Fig. 3, Fig. 4 illustrates the thermomagnetic behavior of a slightly larger Fe_3O_4 particle that has a rhombohedral shape and a major axis of ~250 nm (Fig. 4a). The room temperature magnetic state of this particle is a large clockwise spiraling



vortex with a dipole-like stray magnetic field external to the grain (Fig. 4b). On increasing the temperature to 500 °C, the magnetic contours broaden as the magnetic intensity decreases (Fig. 4c).

Heating to 600 °C (above the Curie temperature (T_c) of ~580 °C) then results in complete demagnetization (Fig. 4d). The vortex state is recovered on cooling back to 500 °C (Fig. 4e) and its magnetic intensity increases upon cooling to 20 °C (Fig. 4f). However, the vorticity then flows in the opposite (counter-clockwise) direction after demagnetization.

This *in situ* TEM off-axis EH investigation provides fundamental insight into the effects of temperature on remanent magnetization in individual Fe_3O_4 PSD grains. The two grains described above display vortex domain structures at room temperature, but different thermomagnetic behaviors on heating close to their T_c of ~580 °C. It is evident that grain size plays an important role in their thermomagnetic response.

At elevated temperature, the 'unblocking' of a stable state and subsequent transition to a lower energy magnetic domain structure depends on competing magnetic energies, which are strongly dependent on grain volume and shape. The magnetization of the vortex structure in the larger grain is more stable at elevated temperature than that of the smaller grain, the key point being that a smaller vortex state grain unblocks and transitions at a lower temperature. SD grains are considered to be the most reliable magnetic recorders. As their grain size increases, they unblock at higher temperatures approaching T_c . This study demonstrates that even small vortex state grains, which were previously considered to be non-ideal magnetic

recorders, recover both their directional and their intensity information after heating close to T_c . The spontaneous recovery of the vortex core in the larger grain (Fig. 4) along the same axis is likely to be influenced slightly by a combination of shape anisotropy and the weak ambient field of < 0.2 mT. The magnetic signal recorded by such a vortex state can, in this instance, assume four possible variations: (1) clockwise or (2) counter-clockwise vorticity, with the direction of the vortex core axis pointing either (3) upwards or (4) downwards out-of-plane. Off-axis EH is limited to measuring the in-plane magnetic component. Hence, the direction of the vortex core is unknown in this instance. The core direction could be determined by acquiring an off-axis EH tilt series, and indeed the entire thermomagnetic behavior in 3D. However, such a measurement is currently both experimentally challenging and computationally demanding. Since the directional information is recovered along the vortex core axis, which can assume only one of two possible orientations, the particle can be said to behave like a uniaxial SD particle at temperatures approaching T_c .

SUMMARY AND CONCLUSIONS

Off-axis EH is a powerful TEM method that can be used to image the magnetic properties of nanoscale materials. This article focuses on the visualization of vortex state magnetic domains in Fe_3O_4 grains. By combining off-axis EH with modern *in situ* capabilities, including controlled heating in vacuum or in the presence of reactive gases with minimal sample drift, it is possible to image the effects of external stimuli on the localized and dynamic magnetism of nanostructures directly.

The combination of off-axis EH

FIGURE 4 Off-axis electron holography of the thermomagnetic behavior of a small Fe_3O_4 grain. (a) Bright field TEM image of an individual Fe_3O_4 particle (major axis ~250 nm). (b-f) Magnetic induction maps recorded (b) at 20 °C (the arrow labelled FD shows the direction of the saturating magnetic field applied to induce remanence) and during *in situ* heating to (c) 500 °C and (d) 600 °C, as well as upon cooling to (e) 500 °C and (f) 20 °C.

and environmental TEM shows that oxidation, which is confirmed using EELS, can change both the strength and the direction of a magnetic vortex state in an individual Fe_3O_4 grain, or in a group of interacting Fe_3O_4 grains. Oxidation may therefore destroy any magnetic information that was carried by original unaltered particles. In contrast, by combining *in situ* heating with off-axis EH, it has been shown that remanent vortex state Fe_3O_4 grains are remarkably stable to thermal effects, with only the magnetic states of smaller Fe_3O_4 grains behaving dynamically at temperatures approaching T_c . In both cases, the combination of off-axis EH with *in situ* TEM techniques provides spatially resolved magnetic information from individual Fe_3O_4 grains, which has previously been inaccessible.

Challenges remain in reconstructing 3D magnetization at every oxidation or temperature interval. Comparisons between experimental magnetic induction maps and simulated induction maps derived from multi-phase 3D micromagnetic models could, in the future, be used to elucidate the 3D nature of dynamic magnetism. Furthermore, advances in MEMS-based *in situ* heating gas cell specimen holders can be used to reconstruct the true remanent magnetic behavior of chemically altered samples without needing to transfer samples between TEMs that have different capabilities.

Article and references available online at: [Microscopy-analysis.com/article/march_19/holography_of_magnetic_minerals](https://doi.org/10.1111/micro.12151)

Microscopy and Analysis 33(2): 12-15 (EU), March 2019

©John Wiley & Sons Ltd, 2019